

Two-Dimensional Electron Magnetohydrodynamic Turbulence

D. Biskamp*

National Institute for Fusion Science, Nagoya 464-01, Japan

E. Schwarz

Max-Planck-Institute fuer Plasmaphysik, 85748 Garching, Germany

J. F. Drake

Institute for Plasma Research, University of Maryland, College Park, Maryland 20742

(Received 13 November 1995)

A novel type of turbulence, which arises in 2D electron magnetohydrodynamics, is studied by numerical simulation. Energy dissipation rates are found to be independent of the dissipation coefficients. The energy spectrum E_k follows the basic Kolmogorov-type predictions, $k^{-5/3}$ for $kd_e > 1$ and $k^{-7/3}$ for $kd_e < 1$ (d_e is the electron inertial length) and is hence independent of the linear wave properties. Results are compared with other 2D turbulent systems.

PACS numbers: 52.35.Ra, 47.27.Eq, 52.30.-q

Two-dimensional turbulent systems have recently attracted considerable attention, notably in Navier-Stokes theory (e.g., [1,2]), magnetohydrodynamics (e.g., [3]), and the Hasegawa-Mima equation (e.g., [4,5]). Apart from their relevance for modeling important predominantly two-dimensional phenomena, such 2D systems are also interesting in their own right. Because of the presence of several ideal invariants 2D turbulent systems exhibit both direct and inverse spectral cascades, the latter giving rise to large-scale self-organization. Here we present results on a novel 2D turbulent system, 2D electron magnetohydrodynamic (EMHD) turbulence. EMHD [6] provides a fluid description of the plasma behavior on scales below the ion inertial length c/ω_{pi} , where the plasma dynamics is governed by electron flows and their self-consistent magnetic fields, while the ions form a static charge-neutralizing background. Special interest in EMHD has arisen to model collisionless reconnection, which appears to be the origin of strong magnetic activity in nearly collisionless plasmas such as the solar corona and the Earth's magnetosphere.

3D EMHD simulations have revealed that strong turbulence is excited by the current density gradients in the reconnection region, which gives rise to anomalous electron viscosity [7]. However, 3D turbulence simulations are still rather limited in spatial resolution. 2D EMHD simulations of the coalescence of two magnetic flux bundles show [8] that the reconnection rate is independent of the smallness parameters of the system, i.e., the electron inertial length c/ω_{pe} and the dissipation coefficients. For sufficiently small values of the latter strong turbulence develops also in the 2D system. In this Letter freely decaying 2D isotropic homogeneous EMHD turbulence is investigated by high-resolution numerical simulations, revealing a number of very interesting properties, which differ from those in previously studied 2D systems.

As in the case of 2D incompressible MHD the 2D EMHD equations can be written in terms of two scalar quantities, the flux function ψ describing the magnetic field in the plane (or poloidal field) $\vec{B} = \hat{z} \times \nabla\psi$, and a stream function φ describing the poloidal electron flow $\vec{v} = \hat{z} \times \nabla\varphi$, which is proportional to the poloidal current density, hence φ gives the out-of-plane or axial field fluctuation $\varphi = \delta B_z$,

$$\partial_t(\psi - d_e^2 j) + \vec{v} \cdot \nabla(\psi - d_e^2 j) = -\mu_\nu(-\nabla^2)^\nu \psi, \quad (1)$$

$$\partial_t(\varphi - d_e^2 a) - d_e^2 \vec{v} \cdot \nabla a + \vec{B} \cdot \nabla j = -\mu_\nu(-\nabla^2)^\nu \varphi, \quad (2)$$

$$j = \nabla^2 \psi, \quad a = \nabla^2 \varphi.$$

The equations are written in nondimensional form using the units L is the typical macroscopic spatial scale, $t_w = (d_e^2 \Omega_e)^{-1}$ is the so-called whistler time, where $d_e = c/\omega_{pe} L$, $\Omega_e = eB_0/m_e c$, and B_0 is the typical (poloidal) magnetic field. [Since in EMHD the ions are assumed infinitely heavy, the Alfvén time $t_A \rightarrow \infty$ cannot be used as a time unit. For finite ion mass we have the relation $t_w = t_A L/(c/\omega_{pi})$.] The density is assumed constant $n = n_0 = 1$, which is consistent with the incompressibility of the electron flow $\nabla \cdot \vec{v} = \vec{\nabla} \cdot \vec{j} = 0$. Including a finite density gradient gives rise to interesting effects in low density plasma opening switches, see, e.g., [6,9], but such effects will not be considered in the present paper. We have also introduced generalized dissipation operators with $\nu = 1$ corresponding to resistivity and $\nu = 2$ to electron viscosity. The ideal invariants of the system (1) and (2) are

$$E = \frac{1}{2} \int \{(\nabla\psi)^2 + \varphi^2 + d_e^2 [j^2 + (\nabla\varphi)^2]\} d^2x, \quad (3)$$

$$H = \int f(\psi - d_e^2 j) d^2x, \quad (4)$$

$$K = \int (\varphi - d_e^2 a) g'(\psi - d_e^2 j) d^2 x, \quad (5)$$

where f and g are arbitrary functions. In turbulence theory the quadratic invariants are most important leading to the choice $f(x) = g(x) = x^2$. Expressions (3)–(5) are generalizations of the corresponding ones in 2D MHD. As in MHD one expects a direct cascade of the energy and an inverse cascade of the (generalized) mean square magnetic potential H . Equations (1) and (2) are more complicated than 2D MHD, containing the inherent scale length d_e . Hence one has to distinguish between the long-wavelength regime $kd_e < 1$ and the short-wavelength regime $kd_e > 1$, though certain properties are found to be uniformly valid.

Linearizing Eqs. (1) and (2) about a constant magnetic field yields the dispersion relation

$$\omega = \pm k k_{\parallel} d_e^2 \Omega_e / (1 + d_e^2 k^2), \quad (6)$$

which corresponds to whistler waves coupling ψ and φ ,

$$\varphi_{\vec{k}} = \pm k \psi_{\vec{k}}, \quad (7)$$

valid independent of $d_e k$. Hence the magnetic field in the large energy-containing eddies gives rise to a coupling of the small-scale poloidal and axial field fluctuations, such that these tend to behave as whistler waves, which we can call the whistler effect in analogy to the Alfvén effect in MHD turbulence [10]. Contrary to Alfvén waves, however, whistler waves are dispersive with large group velocity $v_g \propto k$ for $kd_e < 1$ and $v_g \approx 0$ for $kd_e > 1$. Hence the whistler effect should be strongest for $kd_e \leq 1$. Because of the dispersion properties EMHD cannot be written in terms of the whistler variables $\varphi_{\vec{k}} \pm k \psi_{\vec{k}}$ as is done in MHD by introducing the Alfvén wave variables $\vec{z}^{\pm} = \vec{v} \pm \vec{B}$, the so-called Elsaesser fields. In the latter case the MHD equations show explicitly that only counterpropagating Alfvén waves couple, which is the formal basis of the Alfvén effect leading to the $k^{-3/2}$ energy spectrum [3,10].

Equations (1) and (2) are solved on a quadratic box of size $2\pi \times 2\pi$ with periodic boundary conditions, using a pseudospectral method with N^2 collocation points and dealiasing by the 2/3 rule. N is chosen such as to provide adequate spatial resolution, N varying between 512 and 4096. Initial conditions are $\psi_{\vec{k}} = \exp(-k^2/2k_0^2 + i\alpha_{\vec{k}})$, $\varphi_{\vec{k}} = \exp(-k^2/2k_0^2 + i\beta_{\vec{k}})$, where $k^2 = k_x^2 + k_y^2$, $k_{x,y} = \pm 1, \pm 2, \dots$, $\alpha_{\vec{k}}, \beta_{\vec{k}}$ are random phases, and the dominant initial wave number is $k_0 = 5$. We consider both the case of large $d_e \sim 1$ and small $d_e \ll 1$. In both cases the initial spectrum is concentrated on the lower k side, giving primarily rise to direct cascade processes, though the inverse cascade of H is also clearly visible. Concerning the dissipation operators we usually choose $\nu = 3$ in order to concentrate dissipation at the smallest scales. For $\nu = 2$ results are found to be very similar, while $\nu = 1$ corresponding to a friction term at high k is in general not sufficient to prevent the formation of singular current density gradients.

After an initial relaxation, corresponding primarily to the buildup of small-scale dissipative mode amplitudes, the system soon reaches a self-consistent turbulent state. The energy dissipation rate $\varepsilon = -dE/dt$ rapidly increases up to a maximum value. Subsequently the turbulence and hence ε decay in a self-similar way. An important result is that ε is independent of the dissipation coefficient, as shown in Fig. 1, where the time evolution $\varepsilon(t)$ is plotted for different values of μ_3 . Figure 1(a) refers to $d_e = 0.3$. Shown are three cases, $\mu_3 = 10^{-8}$ (dashed line), 10^{-9} (dash-dotted line), and a case starting with 10^{-8} , switching to 10^{-9} at $t = 0.5$ and to 10^{-10} at $t = 1.0$ (solid line). Turning down μ_3 the system responds by exciting smaller scales, so that the dissipation rate soon reaches the previous level. Figure 1(b) gives similar plots for $d_e = 0.033$. The dashed curve corresponds to $\mu_3 = 10^{-8}$, switches to 10^{-9} at $t = 0.5$ and 10^{-10} at $t = 1$. At $t = 1.4$ μ_3 is switched to 10^{-11} (dash-dotted line).

The energy dissipation rate, however, depends on d_e as is clear comparing Figs. 1(a) and 1(b). We find $\varepsilon(t) \approx (1/d_e)E_0'(t/d_e)$, i.e., $E(t) = E_0(t/d_e)$. This behavior can be derived from Eqs. (1) and (2) in the large- d_e limit. For small d_e , $\varepsilon(t)$ should be independent of d_e , as is, in fact, observed by comparing ε with $d_e = 0.033$ and $d_e = 0.01$ (not shown in Fig. 1).

The energy spectrum E_k , defined by $E = \int E_k dk$, exhibits different power laws for $kd_e > 1$ and $kd_e < 1$. In the former range we find an almost exact Kolmogorov spectrum, as shown in Fig. 2(a). Evaluating different turbulent states we obtain the proportionality constant,

$$E_k = C\varepsilon^{2/3}k^{-5/3}, \quad C = 1.8 \pm 0.1. \quad (8)$$

Since in the range $kd_e > 1$ time scales associated with the linear whistler mode interaction become longer than the nonlinear eddy scrambling time, the Kolmogorov energy transfer process should dominate leading to the spectrum

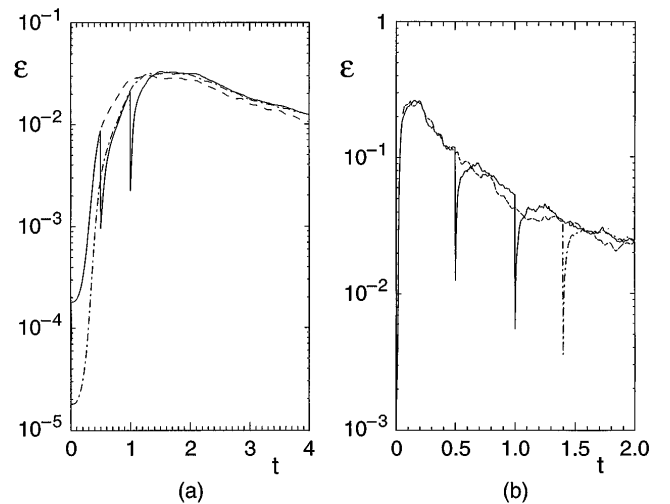


FIG. 1. Energy dissipation rates for different values of μ_3 ; for details see text. (a) $d_e = 0.3$; (b) $d_e = 0.033$.

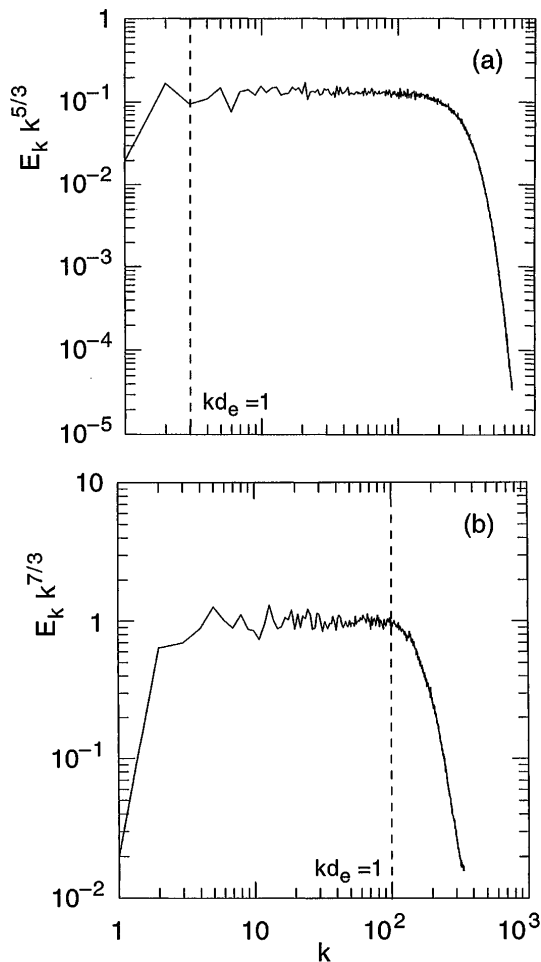


FIG. 2. Compensated energy spectra: (a) $k^{5/3}E_k$ for $d_e = 0.3$; (b) $k^{7/3}E_k$ for $d_e = 0.01$.

(8). It is noteworthy to point out that this spectral law is found to be valid for the entire range $kd_e > 1$ and not only asymptotically for $kd_e \gg 1$.

In the opposite case $kd_e < 1$ the energy spectrum is somewhat steeper [see Fig. 2(b)],

$$E_k \propto k^{-\alpha}, \quad \alpha = 2.25 \pm 0.1. \quad (9)$$

This spectral law can be compared with theoretical predictions. Neglecting the whistler effect we can use a Kolmogorov-type analysis. The eddy interaction time for eddies of scale l is $\tau_l = l/v_e \sim l^2/\varphi_l$. Hence the energy transfer rate becomes $\varepsilon \sim E_l/\tau_l \sim \varphi_l^3/l^2$, from which follows $E_k \sim \varepsilon^{2/3}k^{-7/3}$, using $E_k = k^2|\psi_k|^2 + |\varphi_k|^2 \sim |\varphi_k|^2$. If on the contrary the whistler effect is dominant, the energy transfer, consisting of many weak encounters of oppositely traveling wave packets, is reduced leading to a flatter spectrum, which can be obtained in the following way. The whistler interaction time is $\tau_w \sim l/v_g(l) \sim l^2/d_e^2\Omega_e$. During this time the energy change is $\Delta E_l \sim \varphi_l^2\tau_w/\tau_l$, while the energy transfer time is $\tau_E \sim (E_k/\Delta E_l)^2\tau_w \sim l^2d_e^2\Omega_e/\varphi_l^2$. Hence $\varepsilon \sim \varphi_e^2/\tau_E \sim \varphi_e^4/l^2d_e^2\Omega_e$ and finally $E_k \sim (\varepsilon d_e^2\Omega_e)^{1/2}k^{-2}$. The simulation result (9) tending toward the $k^{-7/3}$ law indicates that even in

the range $kd_e < 1$, where wave propagation effects are strong, they do not dominate the spectral transfer process, though they are sufficient to establish quasiequipartition of poloidal and axial field energies $k^2|\psi_k|^2 \sim |\varphi_k|^2$ in this range.

The most conspicuous spatial structures are those of j and a on the dissipation scale $l_\mu \ll d_e$. Starting from a smooth configuration current and vorticity sheets of length d_e and width l_μ are generated. As discussed in a previous paper [8] these are different from Sweet-Parker sheets in resistive MHD; in particular, the outflow velocity v_0 equals the axial current density in the sheet, the change of the magnetic field across the sheet being negligible. Hence the strongly collimated outflow along the sheet is Kelvin-Helmholtz unstable, which is the origin of the strong turbulence in 2D EMHD. Long sheets break up into shorter ones, thereby spinning off monopolar vortices. The fully developed turbulence [see Fig. 3(a)] is characterized by double layer vorticity sheets and isolated circular monopolar vorticity eddies, both of which are constantly annihilated and reformed. While 2D MHD turbulence consists of microcurrent sheets alone, 2D Navier-Stokes and HM turbulence consist of isolated vortices. Though at small scales the Lorentz force term $\vec{B} \cdot \nabla j$ in Eq. (2) is much smaller than the convective term $\vec{v} \cdot \nabla a$, it is nevertheless important as a source of vorticity. Switching off this term in the state shown in Fig. 3, the vorticity sheets rapidly decay leaving the system in a weakly dissipative state of isolated vortices, which is characteristic of 2D Navier-Stokes turbulence.

In conclusion, we have presented a novel turbulence system, that of 2D EMHD. The most important results are

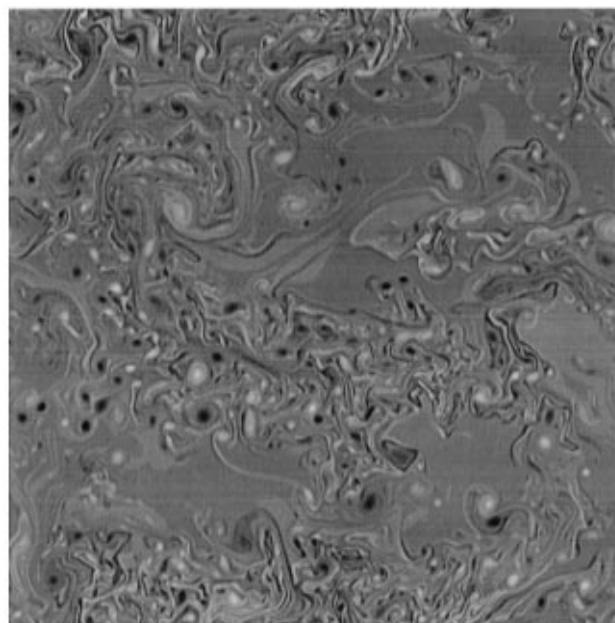


FIG. 3. Grey-scale plots of a for a typical fully developed turbulent EMHD state.

as follows: (a) the energy dissipation rate is independent of the value of the dissipation coefficient; (b) the energy spectrum is $E_k \sim k^{-5/3}$ for $kd_e > 1$ and $k^{-7/3}$ for $kd_e < 1$, consistent with the results of a Kolmogorov-type analysis. Hence the linear wave properties, in particular, the whistler effect, is not important to determine the spectral transfer in contrast to the Alfvén effect in MHD turbulence. It should also be noted that the 2D EMHD turbulence is the first 2D system discussed exhibiting a Kolmogorov energy spectrum.

D.B. acknowledges the support of the COE program (Monbusho) as visiting professor at NIFS Nagoya, where this work was completed.

*On leave from Max-Planck-Institute fuer Plasmaphysik, 85748 Garching, Germany.

- [1] M. Brachet, M. Meneguzzi, H. Politano, and P. Sulem, *J. Fluid Mech.* **194**, 333 (1988).
- [2] L.M. Smith and V. Yakhot, *Phys. Rev. Lett.* **71**, 352 (1993).
- [3] D. Biskamp and H. Welter, *Phys. Fluids B* **1**, 1964 (1989).
- [4] V.D. Larichev and J.C. McWilliams, *Phys. Fluids A* **3**, 938 (1991).
- [5] N. Kukharkin, S.A. Orszag, and V. Yakhot, *Phys. Rev. Lett.* **75**, 2486 (1995).
- [6] A.S. Kinsep, K.V. Chukbar, and V.V. Yan'kov, in *Reviews of Plasma Physics* (Consultants Bureau, New York, 1990), Vol. 16.
- [7] J.F. Drake, R.G. Kleva, and M.E. Mandt, *Phys. Rev. Lett.* **73**, 1251 (1994).
- [8] D. Biskamp, E. Schwarz, and J.F. Drake, *Phys. Rev. Lett.* **75**, 3850 (1995).
- [9] J.D. Huba, *Phys. Plasmas* **2**, 2504 (1995).
- [10] R.H. Kraichnan, *Phys. Fluids* **8**, 1385 (1965).